Appl. Magn. Reson. 25, 599–610 (2004)

Applied Magnetic Resonance

Surface-NMR Relaxation and Echo of Aquifers in Geomagnetic Field

O. A. Shushakov[1,2] and V. M. Fomenko[1]

[1] Institute of Water and Ecological Problems, Institute of Chemical Kinetics and Combustion, Russian Academy of Sciences, Novosibirsk, Russian Federation
[2] Novosibirsk State University, Novosibirsk, Russian Federation

Received August 14, 2003; revised October 29, 2003

Abstract. Macroscopic samples of near-surface water in pores or fractures of rocks down to 100 m and deeper are studied by the measurement of proton relaxation and echo in the Earth's magnetic field. The excitation and reception of the surface nuclear magnetic resonance (SNMR) signal is accomplished with the help of an antenna, circle or 8-shaped (for the minimization of the outer electromagnetic jamming influence), placed at the surface. The frequency of magnetic resonance in the case considered amounts to several kilohertz, the dead time of the instrumentation to several milliseconds. Water in extremely small pores of water-resisting rocks (e.g., in argillaceous grounds), is chemically bound, crystallization or frozen water has smaller times of spin relaxation and is not registered. The distribution of water concentration with depth is determined by inversion of an integral equation, including the model and measured dependences of the SNMR signal against the intensity of excitation. The current state of the art of the SNMR sounding and perspectives of this method on the basis of free induction decay and spin echo detection and relaxation times measurement are presented. Free induction decay T_2^* equal to 60 ms, spin-echo T_2 equal to 220 ms, and inversion-recovery T_1 equal to 700 ms relaxation times have been measured for medium- to coarse-grained sand aquifer. Microscopic characteristics of the aquifer – longitudinal relaxivity ($7 \cdot 10^{-3}$ cm/s), transverse relaxivity ($3.5 \cdot 10^{-2}$ cm/s), and local magnetic field gradient ($2 \cdot 10^{-2}$ G/cm) – have been estimated from experimental data. The importance of spin relaxation and echo measurements for obtaining the information about the microstructure of pores and fractures, as well as filtration properties of aquifers and diamagnetic, paramagnetic and hydrocarbon contamination, is emphasized.

1 Introduction

Soundings by surface nuclear magnetic resonance (SNMR) in the Earth's magnetic field proved to be a rapid and effective method of measuring subsurface movable water content (effective or producible porosity), estimating water-saturated rock pore size (or permeability), and detecting diamagnetic contamination (or salinity). An earlier study [1] discussed some aspects of the SNMR sounding signal of bulk water detected from the ice surface of the Ob reservoir near Novosibirsk. The SNMR experiments of bulk water are useful for calibration and testing of the method. Nevertheless, most of the SNMR applications are devoted to the sound-

ing of near-surface porous or fractured aquifers. The distribution of water saturation down to a depth of 100 m and more is determined by the inversion of an integral equation, including the model and measured SNMR signal amplitude [2]. As it was partly reported earlier [3], the investigation of the set of the spin relaxation times – transverse inhomogeneous spin-spin relaxation time T_2^*, transverse spin-spin relaxation time T_2, and longitudinal spin-lattice relaxation time T_1 – is important to obtain information about the microstructure of pores and to detect diamagnetic, paramagnetic and hydrocarbon contamination. A novel SNMR technique allowed the T_2^*, T_2 and T_1 measurement for medium- to coarse-grained sand aquifers by one- or two-pulse (spin-echo or inversion-recovery) sequences. The effect of the pore size distribution, permeability, and groundwater contamination on SNMR relaxation is considered both theoretically and experimentally.

2 Basic Principles of the SNMR Method

A typical scheme of SNMR groundwater sounding and detection of contamination is sketched in Fig. 1. The method is based on the observation of the proton magnetic resonance in the geomagnetic field of hydrogen ^{1}H nuclei of groundwater molecules H_2O.

In the Earth's magnetic field $\mathbf{H}_0$ a macroscopic magnetization $\mathbf{M}_0(\mathbf{r})$ of a unit volume in thermal equilibrium is described by the following equation [4]:

$$\mathbf{M}_0(\mathbf{r}) = n(\mathbf{r})\frac{\gamma^2\hbar^2}{3kT}S(S+1)\cdot\mathbf{H}_0\,,$$

where $n(\mathbf{r})$ is the number of magnetic nuclei per unit volume, $S = 1/2$ is the nuclear spin, $\hbar$ and k are Planck and Boltzmann constants, and T is the temperature.

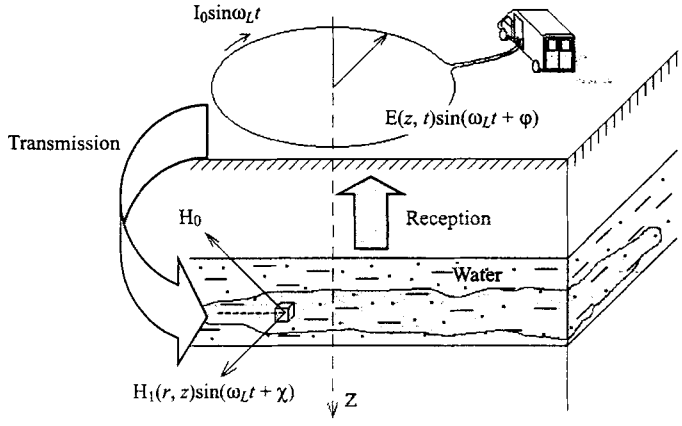

Fig. 1. Scheme of SNMR groundwater sounding and detection of contamination.

After the pulse which generates the oscillating field $\mathbf{H}_1(\mathbf{r}) \cdot \exp(-i\omega t)$, in the resonant case, the frequency ω is equal to the Larmor precession frequency in the geomagnetic field $\omega_L = \gamma_H \cdot \mathbf{H}_0$, the vector $\mathbf{M}_0(\mathbf{r})$ is tilted away from the vector $\mathbf{H}_0$ by the angle

$$\theta(\mathbf{r}) = 0.5 \cdot \gamma_H \cdot H_{1\perp}(\mathbf{r}) \cdot \tau_p , \tag{1}$$

where γ_H is the gyromagnetic ratio of protons, $H_{1\perp}(\mathbf{r})$ is the alternating field component normal to $\mathbf{H}_0$ and τ_p is the pulse duration.

The electromotive force induced in the loop by the magnetic field of groundwater nuclear magnetization is determined by the following equation [1]:

$$E_0(Q) = (\omega / I) \int_V M_\perp(\mathbf{r}) H_{1\perp}(\mathbf{r}) \mathrm{d}V(\mathbf{r}) , \tag{2}$$

where $M_\perp(\mathbf{r}) = M_0(\mathbf{r}) \cdot \sin\theta(\mathbf{r})$, I is the amplitude of the excitation current, $Q = I \cdot \tau_p$ is the excitation pulse intensity (pulse moment), and $E_0(Q)$ is the measured NMR signal amplitude.

The depth of water-saturated layers can be determined from the dependence of the NMR signal amplitude on the excitation-current pulse intensity (the pulse moment) Q.

3 Effect of the Formation of Conductivity

The time-harmonic electric and magnetic fields $\mathbf{E} \cdot \exp(-i\omega t)$ and $\mathbf{H} \cdot \exp(-i\omega t)$ of the loop and groundwater magnetic nuclei are changed in amplitude and phase due to the screening effect of induced currents in the source-free media of magnetic permeability μ, dielectric permittivity ε and conductivity σ.

Assume that the wire loop is placed at the origin of a cylindrical coordinate system (r, φ, z), so that the wire lies along the circle $r = R_0$ in the plane $z = 0$. A homogeneous and uniform formation with conductivity $\sigma_1 = \sigma$ fills the half-space $z > 0$, the air conductivity being $\sigma_0 = 0$. In the half-space $z > 0$, the magnetic field of the loop has the form [5, 6]

$$H_{1z}(\mathbf{r}) = IR_0 \int_0^\infty \frac{m^2}{m+u} \exp(-uz) J_1(R_0 m) \cdot J_0(rm) \mathrm{d}m ,$$

$$H_{1r}(\mathbf{r}) = IR_0 \int_0^\infty \frac{mu}{m+u} \exp(-uz) J_1(R_0 m) \cdot J_1(rm) \mathrm{d}m ,$$

where $u = (m^2 - \varepsilon\mu\omega^2 - i\sigma\mu\omega)^{1/2}$ and J are Bessel functions.

The excitation field $\mathbf{H}_1(\mathbf{r}) \cdot \exp(-i\omega t)$ can be regarded as a complex value in Eq. (2) in the presence of formation conductivity. Equations (1) and (2) can be rewritten as

$$\theta(\mathbf{r}) = 0.5 \cdot \gamma_H \cdot \left|H_{1\perp}(\mathbf{r})\right| \cdot \tau_p ,$$

$$\mathbf{M}_\perp(\mathbf{r}) = \frac{\mathbf{M}_0(\mathbf{r}) \times \mathbf{H}_1(\mathbf{r})}{\left|H_1(\mathbf{r})\right|} \cdot \sin\theta(\mathbf{r}) .$$

The NMR signal also is a complex value with an amplitude and phase. The vector model of the formation of the NMR signal gives the expression [5, 6]

$$E_0(Q) = \frac{\omega}{I} \int_V \frac{M_\perp(\mathbf{r}) H_{1\perp}^2(\mathbf{r})}{\left|H_{1\perp}(\mathbf{r})\right|} \, dV(\mathbf{r}) .$$

The SNMR signal of the loop over the horizontally stratified earth was studied in ref. 7.

4 SNMR Relaxation and Permeability of Porous Rock and Soil

The Darcy law defines the permeability k of a porous medium that governs the flow rate $\mathbf{u}$ of a viscous fluid,

$$\mathbf{u} = k\nabla P/\eta, \tag{3}$$

where ∇P is the pressure drop across the sample, η is the fluid viscosity.

For a liquid, the magnetic relaxation process is coupled with the diffusion of the liquid molecules:

$$\partial M_x/\partial t = D\Delta(M_x - M_{x0}) - M_x/T_{2\text{bulk}} + \gamma(\mathbf{M} \times \mathbf{H})_x , \tag{4}$$

$$\partial M_y/\partial t = D\Delta(M_y - M_{y0}) - M_y/T_{2\text{bulk}} + \gamma(\mathbf{M} \times \mathbf{H})_y , \tag{5}$$

$$\partial M_z/\partial t = D\Delta(M_z - M_{z0}) - M_z/T_{1\text{bulk}} + \gamma(\mathbf{M} \times \mathbf{H})_z , \tag{6}$$

where D is the self-diffusion coefficient, $T_{1\text{bulk}}$ and $T_{2\text{bulk}}$ are the longitudinal and transverse relaxation times of bulk water.

For the presence of an inhomogeneous field, the problem has been treated by Hahn [8], Das and Saha [9], Carr and Purcell [10], Torrey [11], Robertson [12], and others. In the rotating frame ($'$) and with the exponential relaxation factored out of the magnetization [11], it is

$$\partial U/\partial t = D\Delta U - i\gamma GzU , \tag{7}$$

where G is the field gradient, $U = M_x' + iM_y'$, $(\mathbf{n} \cdot \nabla M') = 0$ on the boundary, $\mathbf{n}$ is the unit outward normal directed from the boundary surface.

As a result, the attenuation A by diffusion following a 90° pulse [8–12] is

$$A_{\text{ind}} = \exp(-D\gamma^2 G^2 t^3/3) , \tag{8}$$

the attenuation of the spin-echo amplitude following a 90°–180° pulse sequence is

$$A_{\text{echo}} = \exp(-D\gamma^2 G^2 t^3 / 12). \tag{9}$$

Because NMR lifetimes are related to the lengths that characterize the pore space, magnetic resonance is a valuable noninvasive technique for estimating the permeability of a porous medium. In porous media the fluid's bulk NMR relaxation processes are overwhelmed by the influence of the pore–grain interface, where the proton magnetization decays rapidly due to either the presence of paramagnetic impurities or the hindered rotation of H_2O molecules. The decay is usually described in terms of a phenomenological killing strength ρ [13–15].

The magnetization satisfies the diffusion Eqs. (4)–(6) with the boundary conditions

$$D(\mathbf{n} \cdot \nabla M_x') + \rho_2 M_x' = 0, \tag{10}$$

$$D(\mathbf{n} \cdot \nabla M_y') + \rho_2 M_y' = 0, \tag{11}$$

$$D(\mathbf{n} \cdot \nabla M_z') + \rho_1 M_z' = 0. \tag{12}$$

For the application of the NMR technique to the study of the properties of fluids in porous media, the theoretical studies of Korringa [13] and others resulted in a model of the relaxation of the spin polarization of protons in a hydrogenous fluid in a pore of a solid:

$$1/T_1 = 1/T_{1\text{bulk}} + (S/V)\lambda / T_{1\text{surface}}, \tag{13}$$

where S/V is the ratio of the pore's surface area to its volume, and λ is the thickness of the surface monolayer which by itself would relax with time constant $T_{1\text{surface}}$. For Eq. (13) to hold, diffusion must be fast enough to keep the magnetization uniform across the pore as decay progresses. Equation (13) can be rewritten as

$$1/T_1 = 1/T_{1\text{bulk}} + \rho_1 S/V, \tag{14}$$

where ρ_1 is the longitudinal relaxivity of the surface equal to $\lambda/T_{1\text{surface}}$.

There are three NMR transverse relaxation (T_2) mechanisms for pore fluids in the pore space of a rock: relaxation by bulk fluid processes; grain surface relaxation mechanism; relaxation by molecular diffusion in magnetic field gradients (Eq. (9)):

$$1/T_2 = 1/T_{2\text{bulk}} + \rho_2 S/V + (\gamma G t)^2 D/12, \tag{15}$$

where ρ_2 is the transverse relaxivity Eqs. (10) and (11).

For inhomogeneous transverse relaxation T_2^* there are four NMR relaxation mechanisms for fluids in the pore space of a rock: relaxation by bulk fluid pro-

cesses; grain surface relaxation mechanism; relaxation by molecular diffusion in magnetic field gradients; relaxation due to local magnetic field inhomogeneity:

$$1/T_2^* = 1/T_{2\text{bulk}}^* + \rho_2 S/V + (\gamma G t)^2 D/3 + \gamma G a\,, \tag{16}$$

where a is the pore radius.

Senturia and Robinson [14] and Brownstein and Tarr [15] have considered a model to relate the relaxation time of a liquid-filled porous solid to its geometrical and physical properties. On the basis of such models, Seevers [16], Timur [17–20], Loren and Robertson [21, 22], Kenyon et al. [23, 24], and others estimated the permeability of porous rock from NMR measurements. Kenyon et al. [23, 24] approximated the permeability better by $f^4 T_1^2$ (explained in terms of the presence of throats between pores) than it was by Seevers' classic estimate $f T_1^2$ [16], where f is the porosity and T_1 is the longitudinal relaxation time.

Equations (3)–(16) exhibit different correlations of rock and core permeability and spin relaxation times T_2^*, T_2, T_1.

5 Experimental and Test Sites

The SNMR experiments were performed with the Hydroscope-3 equipment (Institute of Chemical Kinetics and Combustion, Russian Academy of Sciences, Novosibirsk). The technique allows a maximal pulse moment of up to 20000 A · ms (at 40 ms pulse duration) and the possibility of a two-pulse sequence with battery capacitance 0.2 F.

Figure 2 shows the lithological log of well 37 (Novosibirsk) and geophysical logs (resistivity and γ-ray). There was sandy clay aquitard from 0.5 to 21.8 m,

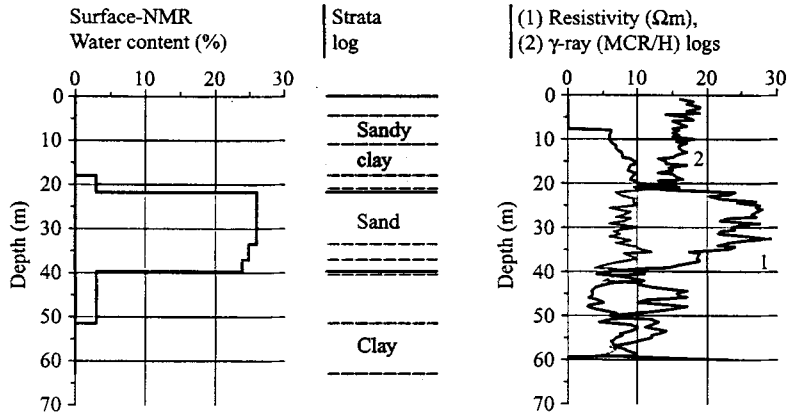

Fig. 2. SNMR water content (%) compared with the strata log, the resistivity, and γ-ray logs for borehole 37 (Novosibirsk site).

medium- to coarse-grained sand aquifer from 21.8 to 39.6 m underlain by clay-rich aquitard from 39.6 to 63 m. The groundwater mineralization (total dissolved solids) at the medium-to-coarse deposit was 0.46 g/l, dissolved Fe ions concentration was about 0.7 mg/l (including Fe^{2+}, 0.3 mg/l). The water permeability coefficient was 379 m^2/day. The resonant frequency of protons measured by the proton magnetometer and by the SNMR technique was 2514 Hz. A 100 m diameter circular loop and an eight-shaped loop [25] had been used at the 37 well.

6 Results and Discussion

Figure 2 compares the SNMR water content with the strata log, the resistivity, and γ-ray logs for the well 37 (Novosibirsk). The SNMR free groundwater content shown in Fig. 2 was obtained by the inversion procedure on the basis of the conjugate-gradient complex-projection algorithm. The strata resolution amounts up to about 1 m at shallower depths and to 10 m and more at close to maximal prospecting depths (down to 100 m and deeper) [2].

The SNMR amplitude and especially the phase are sensitive to the lower resistivity of subsurface material caused by salinity via the effect of electromagnetic screening [5–7]. Figures 3 and 4 compare the SNMR amplitude and phase measured at the well 37 with a 100 m diameter circular loop with the resistivity log calculated for the well 37 (Fig. 2) and for the half-space with the resistivity of 100 Ωm. The porosity $f = 25\%$ (as well as the saturation of groundwater with depth distribution) can be estimated by the inversion procedure (Figs. 2–4).

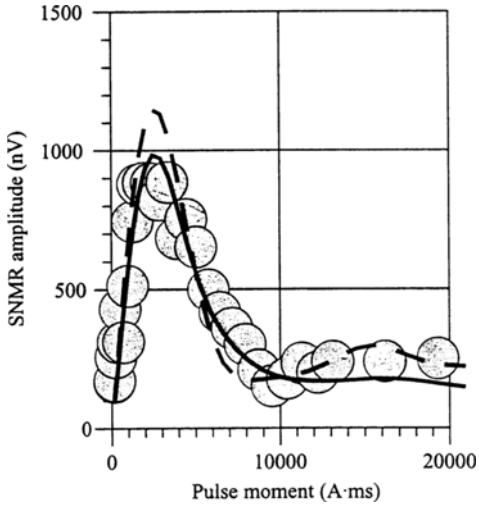

Fig. 3. Comparison of the SNMR amplitude measured at borehole 37 by a 100 m diameter circular loop (circles) with those calculated for the resistivity log of Fig. 2 (solid line) and for half-space with a resistivity of 100 Ωm (dashed line).

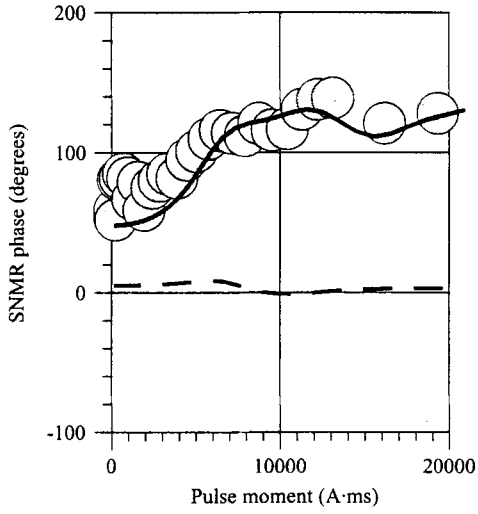

Fig. 4. Comparison of the surface NMR phase measured at borehole 37 by 100 m diameter circular loop (circles) with those calculated for the resistivity log of Fig. 2 (solid line) and for the half-space with the resistivity of 100 Ωm (dashed line).

Figures 5–8 exemplify the SNMR FID and spin-echo amplitudes over time and pulse moment for different time delays between pulses for 16 ms of the first pulse duration and 34 ms of the second pulse duration. We are not aware of any other SNMR experiments that have detected spin echoes of subsurface water.

The spin-echo 90°–180°-pulse sequence has been used for transverse relaxation time T_2 measurement [8]. A standard inversion-recovery 180°–90°-pulse sequence has been used for measuring the longitudinal relaxation time T_1 [26].

Figures 9 and 10 show the transverse and longitudinal spin relaxation times (T_2^*, T_2, T_1), published earlier in ref. 3, measured by the novel technique for the medium- to coarse-grained sand aquifer at the well 37. The relaxation time T_2^* shown in Fig. 9 differs from the phenomenological correlation between inhomogeneous spin-spin relaxation time T_2^* and pore size published earlier [27]. In ref. 27, spin relaxation due to paramagnetic impurities was not taken into account. Figures 9 and 10 within experimental accuracy exhibit the exponential behavior of relaxation curves with decay times $T_2^* = 60$ ms, $T_2 = 220$ ms, and $T_1 = 700$ ms. Spin-spin relaxation times T_2 and T_2^* did not vary with time indicating that the third (diffusion) term in Eqs. (15) and (16) must equal approximately zero for this aquifer. Therefore, the longitudinal relaxivity ρ_1 is equal to $7 \cdot 10^{-3}$ cm/s and the transverse relaxivity ρ_2 is equal to $3.5 \cdot 10^{-2}$ cm/s, as well as the local field gradient equal to $2 \cdot 10^{-2}$ G/cm can be estimated with $T_{1bulk} = 1.4$ s, $T_{1bulk} = 1$ s [3], $a = 2.5 \cdot 10^{-2}$ cm. With the diffusion coefficient $D = 1.3 \cdot 10^{-13}$ cm^2/s for water at 277 K, one can estimate the diffusion term as being equal to $4 \cdot 10^{-10}$ s^{-1} (much less than 1 s^{-1}) in Eqs. (15) and (16), confirming again the approximation made earlier on the basis of the experimental data.

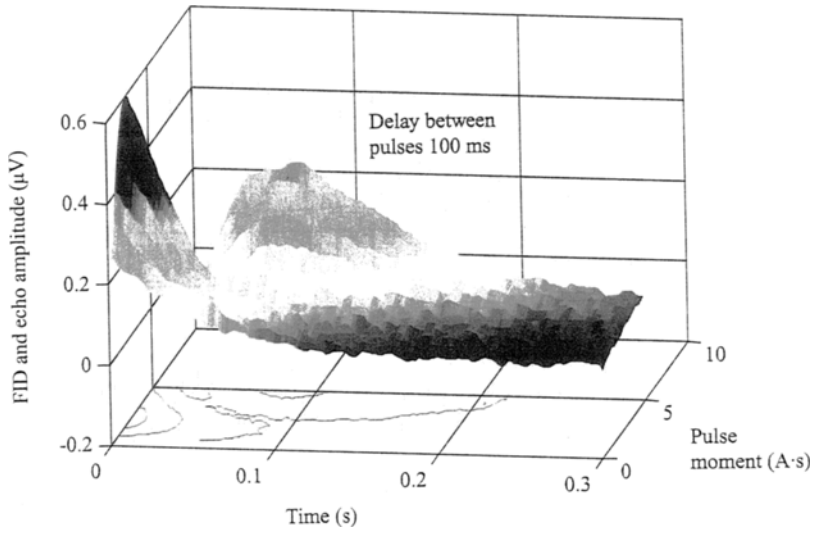

Fig. 5. Surface and contour plot of FID and spin-echo amplitudes over time and pulse moment measured with a pulse sequence with durations of 16 ms (first pulse), 100 ms (delay between pulses) and 34 ms (second pulse) for borehole 37.

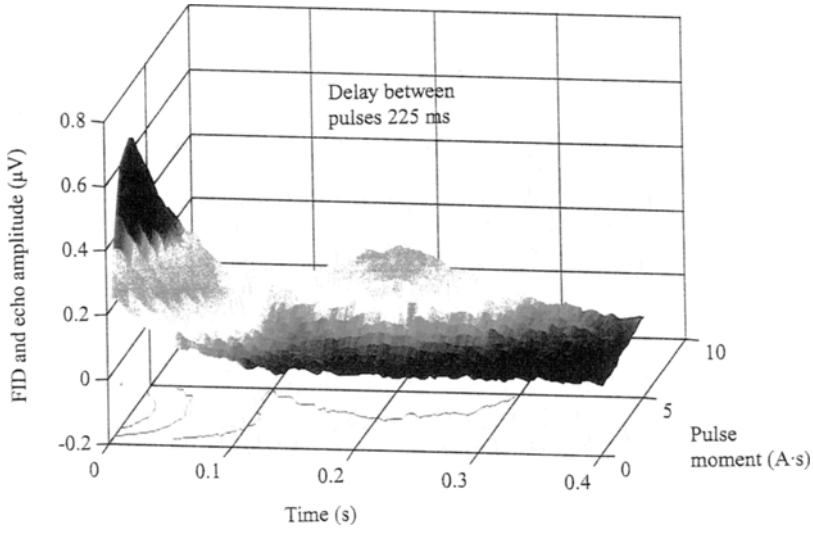

Fig. 6. Surface and contour plot of FID and spin-echo amplitudes over time and pulse moment measured with a pulse sequence with durations of 16 ms (first pulse), 225 ms (delay between pulses) and 34 ms (second pulse) for borehole 37.

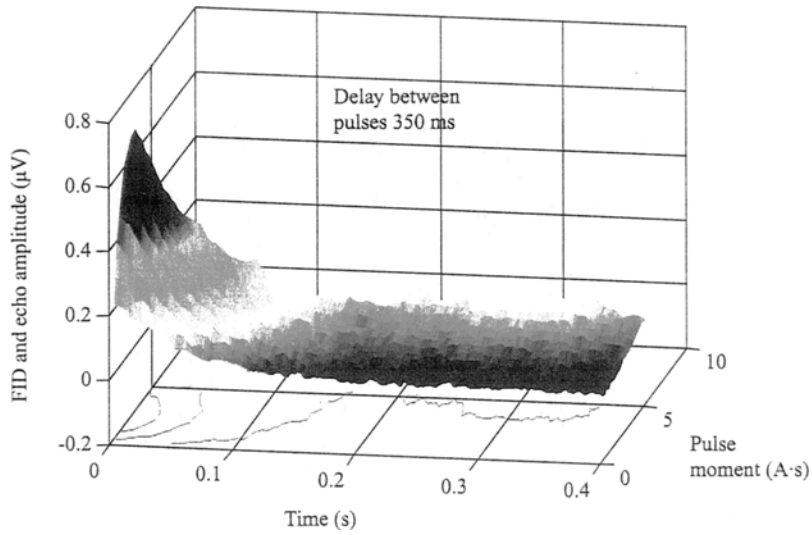

Fig. 7. Surface and contour plot of FID and spin-echo amplitudes over time and pulse moment measured with a pulse sequence with durations of 16 ms (first pulse), 350 ms (delay between pulses) and 34 ms (second pulse) for borehole 37.

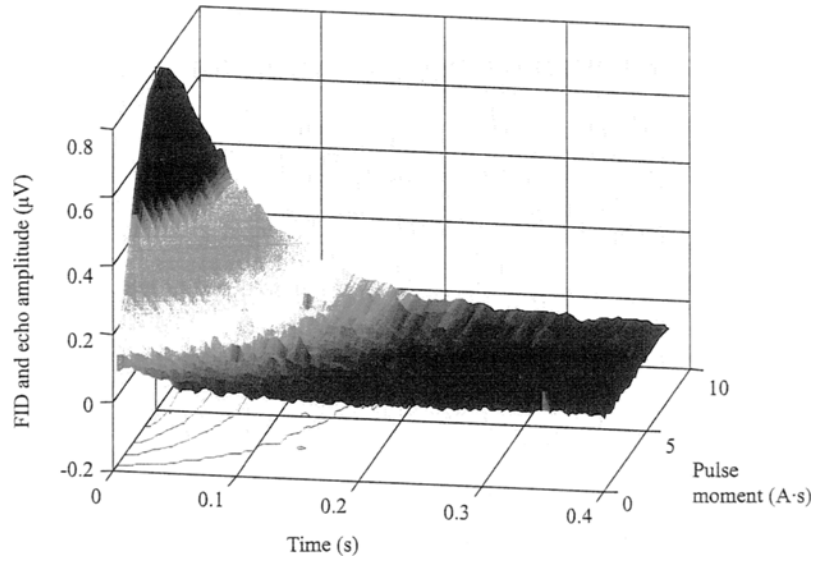

Fig. 8. Surface and contour plot of FID over time and pulse moment measured at 16 ms pulse duration for borehole 37.

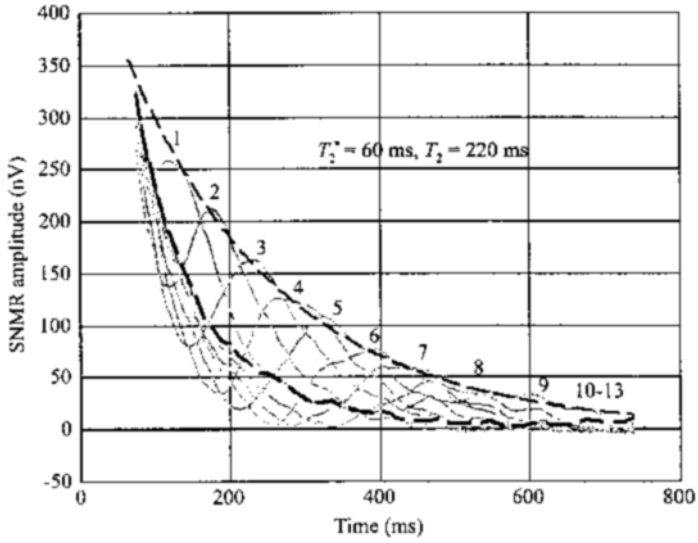

Fig. 9. FID and spin-echo amplitudes measured with pulse sequences with durations of 16 ms for the first pulse (90°) and 34 ms for second pulse (180°) and 100 ms (1) to 700 ms (13) for the delays between pulses with 50 ms intervals between sequences. The transverse relaxation times measured are $T_2^* = 60$ ms and $T_2 = 220$ ms. Borehole 37.

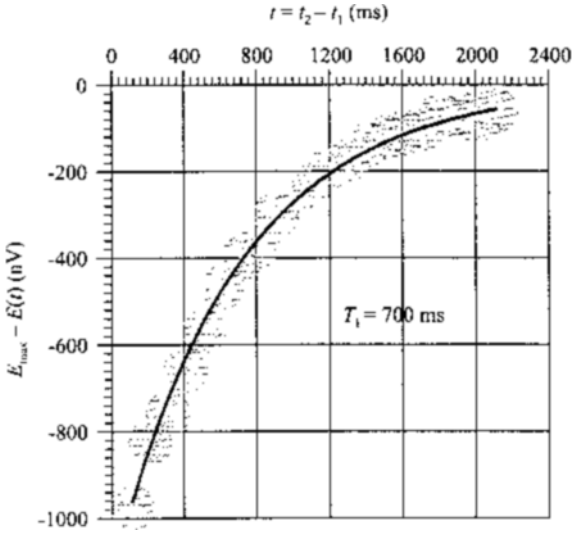

Fig. 10. FID amplitude over time after the second pulse of a pulse sequence with durations of 32 ms for the first pulse (180°), and 18 ms for the second pulse (90°). The longitudinal relaxation time measured is $T_1 = 700$ ms. Borehole 37.

7 Conclusion

A novel SNMR technique allowed the T_2^*, T_2, T_1 measurement for a medium- to coarse-grained sand aquifers with one- or two-pulse (spin-echo or inversion-recovery) sequences. FID T_2^* equal to 60 ms, spin-echo T_2 equal to 220 ms, and inversion-recovery T_1 equal to 700 ms relaxation times have been measured. Such microscopic characteristics of the aquifer as longitudinal relaxivity $\rho_1 = 7 \cdot 10^{-3}$ cm/s, transverse relaxivity $\rho_2 = 3.5 \cdot 10^{-2}$ cm/s, and local magnetic field gradient $G = 2 \cdot 10^{-2}$ G/cm have been estimated from experimental data.

Acknowledgements

We are grateful to Eugene Kalneus, Eiichi Fukushima, Vladimir Novoselov, and Victor Kuskovsky for their assistance in the experiments and fruitful discussion and to the reviewers for the significant improvement of the manuscript.

References

1. Trushkin D.V., Shushakov O.A., Legchenko A.V.: Appl. Magn. Reson. **5**, 399 (1993)
2. Legchenko A.V., Shushakov O.A.: Geophysics **63**, 75 (1998)
3. Shushakov O.A.: Magn. Reson. Imaging **14**, 959 (1996)
4. Abragam A.: The Principles of Nuclear Magnetism. Oxford: Oxford University Press 1961.
5. Shushakov O.A.: Geophysics **61**, 998 (1996)
6. Trushkin D.V., Shushakov O.A., Legchenko A.V.: Geophys. Prospect. **43**, 623 (1995)
7. Shushakov O.A., Legchenko A.V.: Geol. Geofiz. **35**, 161 (1994)
8. Hahn E.L.: Phys. Rev. **80**, 580 (1950)
9. Das T.P., Saha A.K.: Phys. Rev. **93**, 749 (1954)
10. Carr H.Y., Purcell E.M.: Phys. Rev. **94**, 631 (1954)
11. Torrey R.C.: Phys. Rev. **104**, 563 (1956)
12. Robertson B.: Phys. Rev. **151**, 273 (1966)
13. Korringa J.: Bull. Am. Phys. Soc. Ser. II **1**, 216 (1956)
14. Senturia S.D., Robinson J.D.: Soc. Pet. Eng. J. **10**, 237 (1970)
15. Brownstein K.R., Tarr C.E.: Phys. Rev. A **19**, 2446 (1979)
16. Seevers D.O.: Soc. Prof. Well Log. Anal. Symp. Trans. **1966**, paper L (1966)
17. Timur A.: Soc. Prof. Well Log. Anal. Symp. Trans. **1968**, paper K (1968)
18. Timur A.: Log Anal. **10**, 3 (1969)
19. Timur A.: J. Pet. Technol. 775 (June 1969)
20. Timur A.: Soc. Prof. Well Log. Anal. Symp. Trans. **1972**, paper N (1972)
21. Loren J.D., Robinson J.D.: Soc. Pet. Eng. J. **10**, 268 (1970)
22. Loren J.D.: J. Pet. Technol. **24**, 923 (1972)
23. Kenyon W.E., Day P.I., Straley C., Willemsen J.F.: Soc. Pet. Eng. Pap. 15643 (1986)
24. Kenyon W.E., Day P.I., Straley C., Willemsen J.F.: SPE Form. Eval. **3**, 633 (1988)
25. Trushkin D.V., Shushakov O.A., Legchenko A.V.: Geophys. Prospect. **42**, 855 (1994)
26. Fukushima E., Roeder S.B.W.: Experimental Pulse NMR: A Nuts and Bolts Approach. Reading, Mass.: Addison-Wesley 1981.
27. Schirov M.D., Legchenko A.V., Creer J.G.: Explor. Geophys. **22**, 333 (1991)

Authors' address: Oleg A. Shushakov, Institute of Chemical Kinetics and Combustion, Russian Academy of Sciences, Ulitsa Institutskaya 3, Novosibirsk 630090, Russian Federation